

Determination of Lunar Feature Heights from Shadow Lengths

Boris P. Venet

11 Jan 2017

Abstract

We give the details of a method for determining the height or depth of lunar surface features, such as mountains or craters, using measurements of shadow length in a lunar photograph taken through an earth-bound telescope. We apply the method to several feature examples in a photograph captured with a typical amateur telescope and DSLR camera.

1 INTRODUCTION

In the era of spaceflight, accurate measurements of lunar topography heights have been obtained from orbiting lunar probes, using analysis of imagery or, later, laser altimeters. However, without access to NASA and JPL equipment, we can use typical amateur-astronomy equipment to make respectable determinations of the height and depth of prominent lunar mountains and craters, using measurements of shadow lengths in a camera image captured through a small telescope on earth. In this paper, we explain one computational procedure for doing so, and we apply the method to several lunar mountains and craters in a photograph captured with a typical amateur telescope and DSLR camera. The only data required to compute feature-height values in absolute length units are: (i) measurements of image shadow lengths and positions in arbitrary units, and (ii) the radius of the moon in absolute length units.

The basic concept of the calculation is the same as we would use to determine the height of a tall tree in our neighborhood park. The sketch in Figure 1 shows the idea: H is the height of the tree, L is the length of the shadow, and A is the elevation angle of the sun. The relevant trigonometry formula relating the

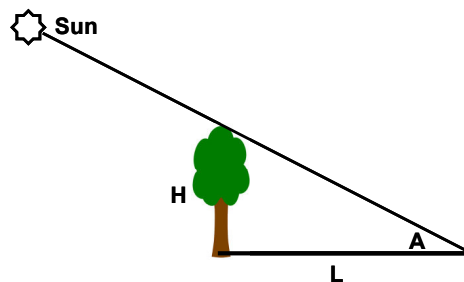


Figure 1: The basic trigonometry concept for height determination

parts of the right triangle is $H = L \cdot \tan(A)$. So, if we measure the shadow length L with a tape measure, and angle A with some version of a protractor, then we immediately obtain H from the tangent formula.

The lunar heights-from-shadows problem uses this same concept, but the details are more complicated, because we're not located near the base of the feature whose height we want to determine. Instead, we must use information from a photo captured at a large distance. The main complications are:

1. We can't position ourselves at the triangle vertex A, so we can't just line up a protractor-type device to measure angle A. We need a more indirect method to determine the sun elevation angle at the location of the feature whose height we want to measure.
2. The mean lunar surface is curved (for present purposes, we can consider it a sphere). Therefore, a shadow length that we measure in the photo is only a fore-shortened version of the shadow length on the surface: in other words, the moon's mean surface in the shadow neighborhood is tilted at some angle with respect to our telescope line of sight.

In Section 2, we give the details of our solution method. In Section 3, we give sample results for several mountains and craters captured in one lunar image. In Section 4, we discuss some error sources and uncertainties in the procedure.

2 IMAGE ANALYSIS AND HEIGHT COMPUTATION METHOD

2.1 Description of the data

We recorded the image data using a Meade 10" telescope, with a Canon DSLR camera (model Rebel T5i) at the Cassegrain focus. The effective focal length was 2032 mm. Figure 2 shows a portion of the image that was used for the height calculations. This image shows a region around Mare Imbrium; name labels point to various craters and mountains that we analyzed. Figure 2 is a cutout of the full camera frame, which is shown in Figure 3. The full frame spans about 0.63×0.42 deg, or 38×25 arcmin, whereas the Figure 2 cutout spans 19×12 arcmin. The full image is needed for one step in the analysis, because we'll need to know where the edge and center of the lunar disk are. The transition from light to dark that runs across the upper left image quadrant is the terminator; the full image, Figure 3, makes this clear.

The key imaging system parameters for present purposes are: effective focal length (EFL) = 2032 mm, camera sensor pixel = $4.3 \mu\text{m}$, hence one sensor pixel subtends $(4.3 \mu\text{m} / 2032 \text{ mm}) = 0.44$ arcsec. Knowing this, the angular distance between any two points in the image plane can be accurately obtained using software that provides pixel-level access to the image data. Then, we can scale any angular separation to absolute distance units (say, meters) if we assume that we know the radius of the moon in meters. The absolute radius value is the only datum that we need, that cannot be obtained from the image itself.

It is also necessary to locate the center of the lunar disk, which functions as a reference point (coordinate origin) for subsequent calculations. For present purposes, a sufficiently accurate way of doing this is by drawing a few perpendiculars to the disk edge, and finding their intersection point; this preliminary step is suggested by the radial lines added to the Figure 3 image.

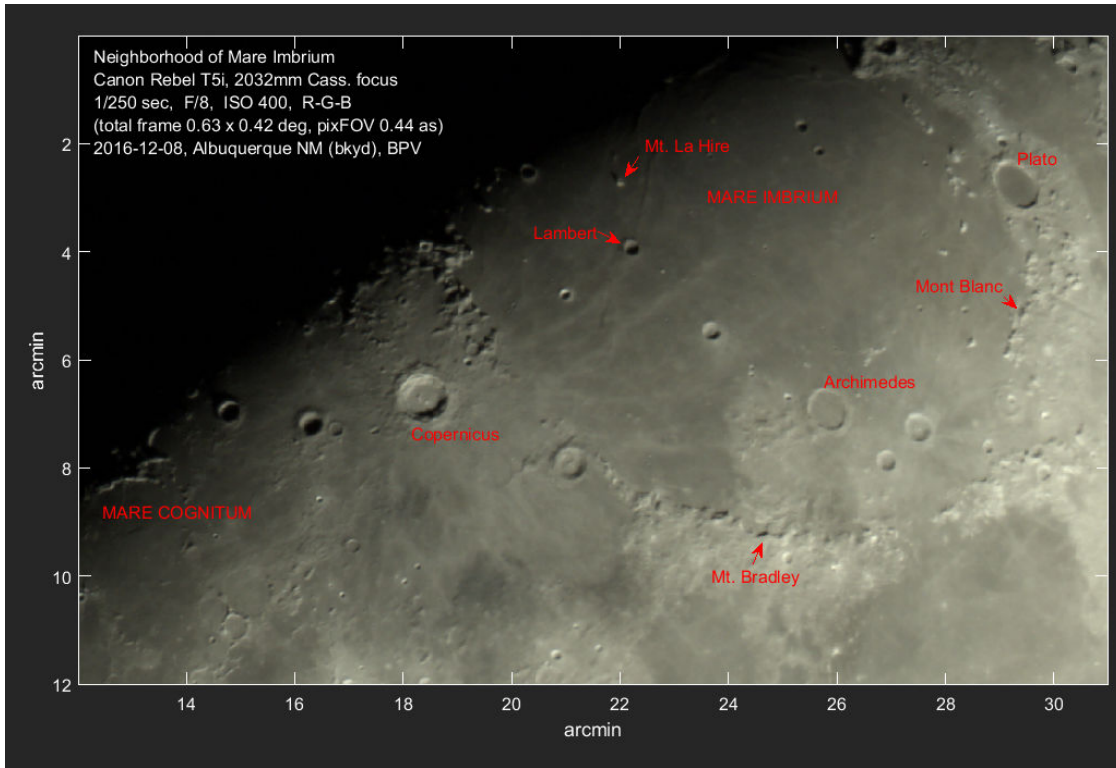


Figure 2: Portion of a lunar image, captured with a Meade 10" telescope, focal length 2032 mm

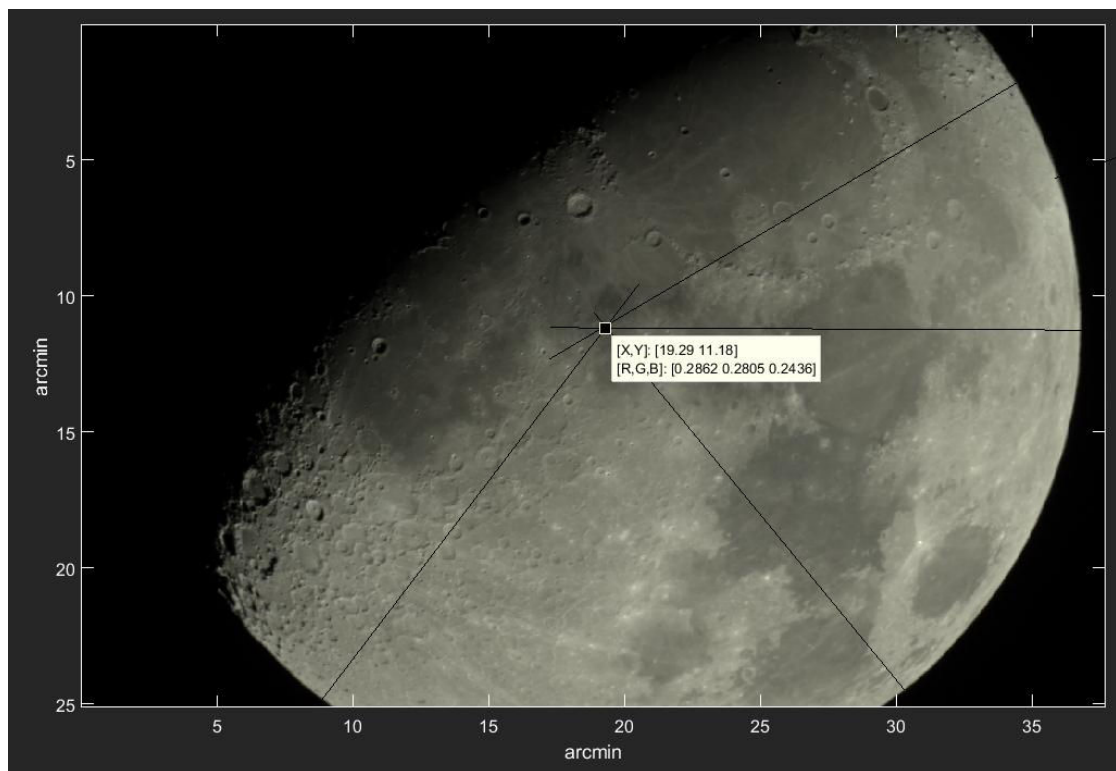


Figure 3: The full camera image, of which Figure 2 is a cutout

2.2 Outline of the analysis procedure

- (A) As noted above, we can use the full image to find the center of the lunar disk. That serves as a key reference point for the calculations. We also assume that we know the radius of the moon, in meters.
- (B) Next, we measure off the photo the location of the center point of the terminator. Using some trigonometry, the distance between the center of the terminator and the center of the lunar disk tells us the angle between the sunlight and the telescope line-of-sight (LOS). (For example, if the distance is zero, i.e., the terminator runs exactly through the disk center, then the angle between sunlight and telescope LOS is 90 deg). The telescope line of sight is perpendicular to the plane of the photo, and, due to the large distance, the image is an orthographic projection of the 3D lunar surface onto the image plane.
- (C) Finally, we go to a feature whose height we want to measure (for example, the height of the labeled Mt. La Hire). From the photo, we measure off the position of the feature (the base of the mountain), and the length (projected, or fore-shortened) of its shadow. Using the location of the feature, trigonometry tells us the orientation of the lunar surface in the neighborhood of the feature. Combining that with the result of step (B), we obtain the solar elevation angle at the feature. More trigonometry gives us a formula that relates the projected shadow length and illumination angle to the feature height; we can solve this equation for the remaining unknown, the desired feature height.

2.3 Analysis details

The mathematical details of the procedure steps B and C can be developed as follows.

Solar illumination angle with respect to telescope line of sight:

Figure 4(a) shows a sketch of the lunar disk and terminator line, and our coordinate system. The x-y axes are parallel to the image plane, and the z axis is parallel to the telescope line of sight. R is the radius of the moon, and segment t is the perpendicular distance from the center of the disk to the terminator. Figure 4(b) is a cross-section through the origin, perpendicular to the page, and containing the point T . We need the angle β , which is the direction of the solar illumination with respect to the z axis. From the geometry of the two triangles, we see that

$$\beta = \cos^{-1}(t/R) \quad (1)$$

For example, $t = 0$, i.e., terminator running exactly through the disk center, corresponds to $\beta = 90$ deg, whereas $t = R$, i.e., full moon, corresponds to $\beta = 0$. (With due attention to sign conventions, the same formalism can be used if the terminator is on the opposite side of the origin.)

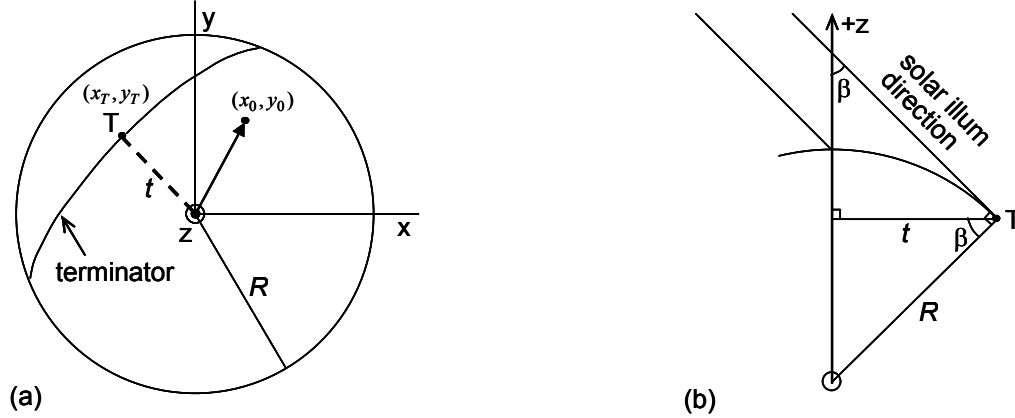


Figure 4: (a) Lunar disk with terminator; (b) Perpendicular slice through origin and point T

It will be useful to also introduce spherical-polar coordinates, where θ is the polar angle of a point with respect to the z axis, and ϕ is the azimuthal angle counter-clockwise from the x axis. The spherical-polar coordinates of the sun, with respect to the coordinate system in the sketch, are

$$\theta_S = \beta \quad , \quad \phi_S = \tan^{-1}(y_T/x_T) + \pi \quad (2)$$

Solar illumination angle with respect to local vertical at selected surface feature:

To analyze the shadow of a selected surface feature, we need the illumination angle γ at that location on the surface. Angle γ will be a function of the angle β and the position of the surface point relative to point T . We designate the x - y coordinates of the selected surface point by (x_0, y_0) , and of the point T by (x_T, y_T) . Assuming that the mean lunar surface is a sphere, the complete Cartesian coordinates of the feature location are (x_0, y_0, z_0) , where $z_0 = \sqrt{R^2 - x_0^2 - y_0^2}$. The spherical-polar coordinates of the surface feature are

$$\theta_0 = \cos^{-1}(z_0/R) \quad , \quad \phi_0 = \tan^{-1}(y_0/x_0) \quad (3)$$

where the inverse tangent should be understood as the four-quadrant version.

The remaining spherical trigonometry is easiest to work out using vector notation, as follows.

At the feature location (x_0, y_0, z_0) on the curved lunar surface, the unit normal vector (the local vertical) can be expressed in Cartesian coordinates as

$$\hat{n}_0 = \sin \theta_0 \cos \phi_0 \hat{x} + \sin \theta_0 \sin \phi_0 \hat{y} + \cos \theta_0 \hat{z} \quad (4)$$

where (θ_0, ϕ_0) are given in terms of measured quantities by Eq. (3). The $\hat{x}, \hat{y}, \hat{z}$ symbols are the Cartesian unit vectors.

Likewise, the unit vector that represent the direction towards the sun is

$$\hat{n}_S = \sin \theta_S \cos \phi_S \hat{x} + \sin \theta_S \sin \phi_S \hat{y} + \cos \theta_S \hat{z} \quad (5)$$

where (θ_S, ϕ_S) are given in terms of measured quantities by Eq. (2).

The local illumination angle γ is the angle between \hat{n}_0 and \hat{n}_S , which is immediately given by the dot product: $\hat{n}_0 \cdot \hat{n}_S = \cos \gamma$. Carrying out the dot product using formulas (4) and (5), we obtain

$$\gamma = \cos^{-1}(\sin \theta_0 \sin \theta_S \cos(\phi_0 - \phi_S) + \cos \theta_0 \cos \theta_S) \quad (6)$$

Relation between feature height, angle γ and measured shadow length:

At this stage, we have angle γ in terms of measured quantities. The remaining problem is to find the relation between the height H of the surface feature, the illumination angle γ , and the measured shadow length. The measured shadow length is the projected length in the x-y plane. Figure 5 shows the relevant diagram: the plane of this sketch is that plane which contains the surface feature point (x_0, y_0, z_0) and the two directions \hat{n}_0 and \hat{n}_S . In other words, this is the plane of incidence of the solar rays at the feature location. The physical shadow of H also lies in this plane, along the surface of course, and is denoted by L in the diagram. This diagram highlights one approximation in our procedure: we assume that over the length of the shadow, the mean surface is planar (i.e., not appreciably curved). We'll comment further on the validity of the approximation in the discussion of Section 4. The relation between H and L is simply $L = H \tan \gamma$.

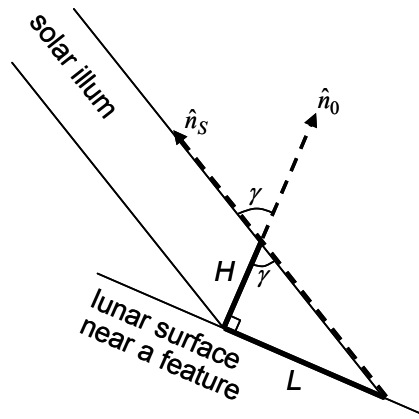


Figure 5: Plane of incidence of solar rays at the surface feature.
(Note: the z axis is not in the plane of this figure)

But now from our photo data, we can only measure the projection of the shadow L that lies in the x-y plane (the image plane): we'll call this projected length L_{xy} . Since the z axis does not lie in the plane of the Figure 5 sketch, the L_{xy} component is a bit difficult to visualize. We can obtain it by using the following vector manipulations. First, we define the shadow vector \vec{L} via the vector cross-product $\vec{L} = L (\hat{n}_S \times \hat{n}_0) \times \hat{n}_0 = H \tan \gamma (\hat{n}_S \times \hat{n}_0) \times \hat{n}_0$. This vector has length L , and points along the surface in the direction of the physical shadow. Since we know the Cartesian components of the right-hand side of the last formula, we can just extract the x and y components, which represent the desired projection of \vec{L} onto the x-y plane. Once that is done, we can invert for H to get our final answer. The details are as follows.

First, it's helpful to expand the triple cross product using a standard vector identity:

$$\begin{aligned} \vec{L} &= H \tan \gamma (\hat{n}_S \times \hat{n}_0) \times \hat{n}_0 \\ &= H \tan \gamma [\hat{n}_0 (\hat{n}_0 \cdot \hat{n}_S) - \hat{n}_S (\hat{n}_0 \cdot \hat{n}_0)] = H \tan \gamma [(\cos \gamma) \hat{n}_0 - \hat{n}_S] \end{aligned} \quad (7)$$

Now, we want the length of the x-y projection, which we've called L_{xy} : we obtain this from Eq. (7) by evaluating

$$\begin{aligned}
 L_{xy} &= \sqrt{L_x^2 + L_y^2} \\
 &= H \tan \gamma \cdot \sqrt{\cos^2 \gamma \sin^2 \theta_0 + \sin^2 \theta_S - 2 \cos \gamma \sin \theta_0 \sin \theta_S \cos(\phi_0 - \phi_S)}
 \end{aligned} \tag{8}$$

To obtain the second line of Eq. (8), we used the components of \hat{n}_0 and \hat{n}_S expressed in Eq. (4) and (5).

Now we simply invert Eq. (8) to yield the final answer for the desired feature height H :

$$H = \frac{L_{xy}}{\tan \gamma \cdot \sqrt{\cos^2 \gamma \sin^2 \theta_0 + \sin^2 \theta_S - 2 \cos \gamma \sin \theta_0 \sin \theta_S \cos(\phi_0 - \phi_S)}} \tag{9}$$

On the right-hand side of Eq. (9), the numerator is the projected shadow length directly measured in the image, and the various angles are also obtained from position coordinates in the image via formulas (2), (3) and (6).

3 SAMPLE RESULTS FOR SOME CRATER DEPTHS AND MOUNTAIN HEIGHTS

We numerically evaluate H , according to Eq. (9), for three mountains heights and three crater depths, for the features labeled in the Figure 2 photograph. All the angle quantities in our formulas are specified in previous formulas as ratios of measured distances in the photo. Therefore, these could be measured off the photo in any convenient units, with a simple ruler from a magnified picture if necessary. Of course in modern times we use a piece of software that gives us pixel-level access to the digitized image, and we can just measure the distances in pixels. Equation (9) then gives us H in pixels, and we can scale that to physical meters if we assume that we know the radius of the lunar disk in meters. This physical radius is the only data value we use that is not obtained from the image itself. Table 1 shows the numerical results for our selected features: “H_bv” are the heights we obtained from our photo measurements, and “H_truth” are best-known values obtained from Wikipedia articles on the individual lunar features. All values are in meters. The truth values were typically obtained by research groups that analyzed imagery or laser-altimeter data obtained by lunar-orbiter probes from close range.

Feature	H_bv (m)	H_truth (m)
Mt. La Hire	1700	1500
Lambert	2300	2700
Copernicus	3930	3800
Plato	1500	1000-1400
Mt. Blanc	2700	3700
Mt. Bradley	4800	4200

Table 1: Comparison of heights determined from the photo with truth values

4 DISCUSSION

With the methods used in this paper, the table shows that our sample results are typically 15%-30% off from the best-known values. Given various uncertainties in the measurement procedure, this is about as good as could be expected. Key uncertainties in the procedure are:

- 1) Given the image resolution, it can be difficult to determine exactly what image pixel represents the base of the selected feature (say a mountain peak).
- 2) When the feature is an extended one, for example a spread-out mountain or a crater rim, there is some uncertainty in determining in what direction the shadow should be measured. In our image, we used Mt. La Hire as a key clue, because of its very isolated nature and long shadow.
- 3) Of course, the procedure is typically less accurate the further away the feature is from the terminator, since the length of the shadow becomes smaller relative to the uncertainties discussed in the previous list items.
- 4) Some height features, such as crater rims, are substantially irregular, and we may not know precisely to which point the truth value refers. For example, for the Plato rim in the table, we give a range of “truth” values.

The obvious way of improving the reliability of the results would be to take multiple photos of a feature, at different sun angles, and then compute best-fits from the multiple measurement results. It would be interesting to do some research in the old astronomy literature, to see exactly what procedures were applied and best results were obtained prior to the space-probe era.

Other than the measurement errors discussed above, our procedure uses a couple of basic physics and mathematical approximations which should have relatively negligible impact. For example, we assumed the lunar surface is a sphere, which is close to the truth but not exactly correct. We also assumed that, over the length of a feature shadow, the surface is not significantly curved. This is an accurate approximation for the shadow lengths that we considered, which are of order 10 km or less. We must also be careful to not apply the procedure (at least its basic version) to features that have specific shapes that obviously violate the local-flatness assumption. For example, some smaller craters may have a bowl-shaped profile with no central flat plain. In such a case, the projected shadow would typically underestimate the height from the deepest point to the shadow-casting rim. Multiple measurements from different sun angles could help to resolve difficult cases like this. A similar minor issue that could occur, for example in the vicinity of mountains, is that the local surface is a reasonably flat but slightly tilted plain.

5 SUMMARY

We have documented the details of a procedure for obtaining the heights of lunar surface features from their shadow lengths. We have applied the method to shadow measurements taken from a lunar photograph captured with a typical amateur-telescope imaging system. We have obtained numerical height and depth values for selected lunar mountains and craters, and discussed the measurement errors and reliability of the results.